Received: 19 March 2020 | Revised: 8 August 2020 | Accepted: 11 August 2020

DOI: 10.1111/bre.12505

ORIGINAL ARTICLE

Basin Research | IAS EAGE | WILEY

Fault-controlled base-of-scarp deposits

Domenico Chiarella[1] | **Walter Capella**[1] | **Sergio G. Longhitano**[2] | **Francesco Muto**[3]

[1]Clastic Sedimentology Investigation (CSI), Department of Earth Sciences, Royal Holloway, University of London, Egham, United Kingdom

[2]Department of Sciences, University of Basilicata, Potenza, Italy

[3]Dipartimento di Biologia, Ecologia e Scienza della Terra, University of Calabria, Italy

Correspondence
Domenico Chiarella, Clastic Sedimentology Investigation (CSI), Department of Earth Sciences, Royal Holloway, University of London, Egham, United Kingdom.
Email: domenico.chiarella@rhul.ac.uk

Abstract

The term base-of-scarp is proposed for those submarine deposits controlled by a fault and physically disconnected from their more proximal counterpart located on the footwall, although genetically linked to it. These systems differ from conventional fault-controlled deltas, such as shoal- and Gilbert-type, because they are entirely subaqueous and lack equilibrium morphology—a steady state in which the system grows in size without altering its shape. We present field examples of fault-controlled deposits from the Crati Basin and the Messina Strait (southern Italy) consisting of stratigraphic clastic wedges that thin towards and onlap onto the active margin with primary inclined bedding. Beds are composed of immature coarse-grained gravels and sand, lack structures representative of wave-action and reflect gravity-driven processes such as debris flow, debris fall and high-density turbidity currents. These deposits represent the unsteady-state phase in which the system grows reducing its slope angle leading to conditions under which the unsteady state may eventually turn into a Gilbert-type or shoal-water system. A diagram for fault-controlled base-of-scarp (B), Gilbert (G) and shoal-water (S) deposits is presented, including their steady- and unsteady states, and the conceptual conditions under which a base-of-scarp system might evolve into Gilbert-type or shoal-water systems and vice versa.

1 | INTRODUCTION

Fault-controlled deposits develop in tectonically active basins forming tens of meters to hundreds of meters thick successions. Usually, the higher the syn-depositional cumulative displacement created by the fault, the thicker the deposit stacks (Hardy, Dart, & Waltham, 1994). Fault-controlled depositional systems have long been studied to improve the understanding and prediction of sand- and gravel-body architectures in analogous subsurface systems (Colella, 1988a; Ethridge & Wescott, 1984; Lewis, Jackson, Gawthorpe, & Whipp, 2015; Longhitano, 2008). Such fault-controlled deposits are important in basin analysis because they provide a record of tectonic events and base level changes that operated during basin evolution (Gobo, Ghinassi, & Nemec, 2015; Hardy et al., 1994). However, existing classification schemes and models for fault-controlled systems (e.g. Massari & Colella, 1988) put little emphasis on the embryonic phase of unsteady-state development. Embryonic phases develop when sediments are (a) sourced along a fault scarp directly into relatively deep-water basins and (b) transported through gravity-driven processes to form wedge-shaped accumulations (Nemec, 1990). The resulting base-of-scarp deposit does not generate sufficient sediment volume to reach base level and to evolve as a delta with a subaerial or shallowly submerged distributary plain (Figure 1). The proposed unsteady state (i.e. base-of-scarp deposit) is characterised by the evolution in morphology and internal geometry during

basin filling (Prior & Bornhold, 1988) gradually reducing its slope angle through time (Nemec, 1990), eventually aggrading close to the base level and potentially evolving into either a shoal-water or Gilbert-type delta system with morphologies that grow in steady-state conditions.

Although in the literature there has been little attention to fault-controlled base-of-scarp deposits, they can be recognised in many syn-rift basins where they characterise their early phases. Accordingly, our understanding of the tectono-stratigraphic evolution is poor despite unsteady base-of-slope deposits contain useful information about basin evolution and development of fault-controlled deposits. The reason why they are poorly studied can be that they are relatively thin compared to other syn- and post-rift deposits, poorly imaged in seismic reflection data and typically included and interpreted within the well-known steady-state deposits in which they evolve.

Deposits referable to base-of-scarp systems have been described in different geological contexts like fjords or tectonically controlled deep environments in outcrop (e.g. Wollaston Forland Group, Greenland) and subsurface examples (e.g. Brae Formation, North Sea), and referred to as underwater conical delta, apron or submarine fan (Ethridge & Wescott, 1984; Henstra et al., 2016; Leeder & Gawthorpe, 1987; Nemec, 1990; Prior & Bornhold, 1988; Surlyk, 1984; Turner & Connell, 2018; Cullen et al., in press). All the previously used terminologies have not found so far a common ground with people indistinctly using different terms for similar systems. Here we suggest to use the term 'base-of-scarp' for all the cases where the system is (a) fault-controlled, (b) represents an unsteady-state embryonic accumulation and (c) can evolve through time to a steady-state system like Gilbert-type deltas or shoal-water accumulation. Syn-rift deposits evolving through unsteady and steady-state phases can be recognised, among others, in published examples of rifted deposit of the Bohai Bay Basin (e.g. Jia et al., 2019), the Crati Basin (e.g. Colella, 1988b) and the Gulf of Suez (e.g. Lewis et al., 2015; Figure 1), although not emphasised by the authors. Moreover, many cases can be hidden in examples where the published iconographic material or description does not easily allow their identification.

In this paper, we investigate fault-controlled base-of-scarp deposits from two study areas (the Plio–Pleistocene Crati Basin and Messina Strait, southern Italy) to document their geometric and sedimentological characters and the transition to steady-state deltas that might occur if sediment accumulation exceeds tectonically created nearshore accommodation. Our hypothesis is that by defining base-of-scarp deposits and comparing them with published models of shoal-water and Gilbert-type delta systems in the literature, we can (a) distinguish features such as internal architecture and facies distribution, and (b) provide a frame of reference for future studies on fault-controlled deposits. We propose a BGS diagram with base-of-scarp (B), Gilbert (G) and shoal-water (S) fault-controlled systems. The diagram includes their initial unsteady state and evolution paths towards steady state. Evolution can potentially go backwards to unsteady state if accommodation outpaces sediment supply producing sub-vertically stacked systems (e.g. Colella, 1988b; Dorsey, Umhoefer, & Renne, 1995; Garcia-Garcia, Fernandez, Viseras, & Soria, 2006). The aim of this paper is to advance our understanding of fault-controlled deposits, and in particular of their embryonic unsteady state. Using field data, the objectives of the study are (a) describe and interpret the base-of-scarp deposits evolution of three fault-controlled deposits exposed at the Civita, San Teodoro and Croce Valanidi sections (southern Italy) from the stratigraphic architecture and sedimentology; (b) propose a ternary diagram showing the evolving though time from the unsteady-state end-member to the steady-state ones and vice versa; (c) discuss the controlling factors of base-of-scarp deposits and their potential evolution to Gilbert-type and shoal-water systems.

Highlights

- We document fault-controlled base-of-scarp deposits and the depositional architectural evolution from unsteady- to steady-state conditions.
- Base-of-scarp deposits represent the embryonic state characterising early extensional phases
- Internal architectures and facies distribution of base-of-scarp deposits characterised by a fining-upward trend differs markedly from the progradational coarsening-upward trend recognised in deltaic successions and alluvial fans
- Depth-ratio and depositional angle control the evolution of fault-controlled systems

2 | FAULT-CONTROLLED SYSTEMS CLASSIFICATION

Classification diagrams are largely used in sedimentology to group depositional environmentals and elements having common characters. Different proposed diagrams cover the spectrum of classical depositional systems (e.g. Boyd et al., 1992; Galloway, 1975, Ainsworth et al., 2003). Fault-controlled Gilbert- and shelf-type deltas and base-of-slope deposits have been recognised and documented in both modern and ancient systems (Colella, 1988a; Galloway, 1988; Massari & Colella, 1988; Nemec, 1990). However, no available classification schemes have been proposed to define or name fault-controlled base-of slope systems typically representing the embryonic phase reflective of an unsteady state. Neither is a model available for the prediction of evolution of these

depositional systems through time and space. Here we develop a triangular diagram for fault-controlled systems showing how base-of-scarp systems may potentially evolve from an initial unsteady state, and evolution paths towards the steady state. The diagram uses discrete categories representing end members. In particular, each of the three vertices of the ternary diagram refers to base-of-scarp (B), Gilbert (G) and shoal-water (S; Figure 2). Base-of-scarp deposits (B) represent the unsteady-state end-member, while Gilbert (G) and shoal-water (S) the steady-state ones. Infinite numbers of mixed systems can exist in between depending on the interaction among sedimentary supply, relative sea level changes and extensional rate. Moving from the top vertex 'B' towards the base of the triangle, systems increase their steadiness evolving though time from the unsteady-state end-member and the steady-state ones and vice versa.

3 | GEOLOGICAL SETTING

3.1 | Tectonics and structure of the Crati Basin and Messina Strait

Our field examples are located in two basins (Crati and Messina, southern Italy, Figures 3 and 4) that were active during the Plio–Pleistocene and associated with the last tectonic displacement of the Calabrian Arc (Monaco & Tortorici, 2000; Tansi, Muto, Critelli, & Iovine, 2007; Van Dijk et al., 2000). The Crati Basin and the Messina Strait represent two extensional basins related to the Late Pliocene–Early Quaternary block segmentation of the Calabrian Arc interpreted as the effect of the migration of the orogen towards the forearc Ionian Basin (Ghisetti, 1979; Tansi et al., 2007; van Dijk et al., 2000).

3.1.1 | The Crati basin

The Crati Basin, which is located in the northern part of the Calabrian Arc, is an L-shaped basin developed since Early-Pleistocene in response to the W-E extension that characterises the western portion of the Calabrian Arc (Figures 3, 4a and 5; Turco, Maresca, & Cappadona, 1990). The Crati Basin trends N-S in the southern portion, with an E-W-oriented component in the northern part (Figure 3b). The basin margin consists of Palaeozoic crystalline rocks of the Sila Massif to the east, crystalline and sedimentary rocks of the Coastal Range to the west and Meso-Cenozoic carbonate deposits of the Pollino Massif to the north. The Crati Basin hosts well-known examples of fault-controlled shoal-water and Gilbert-type deltas (Colella, 1988b), and in the present study we focus on facies variations and vertical evolution of

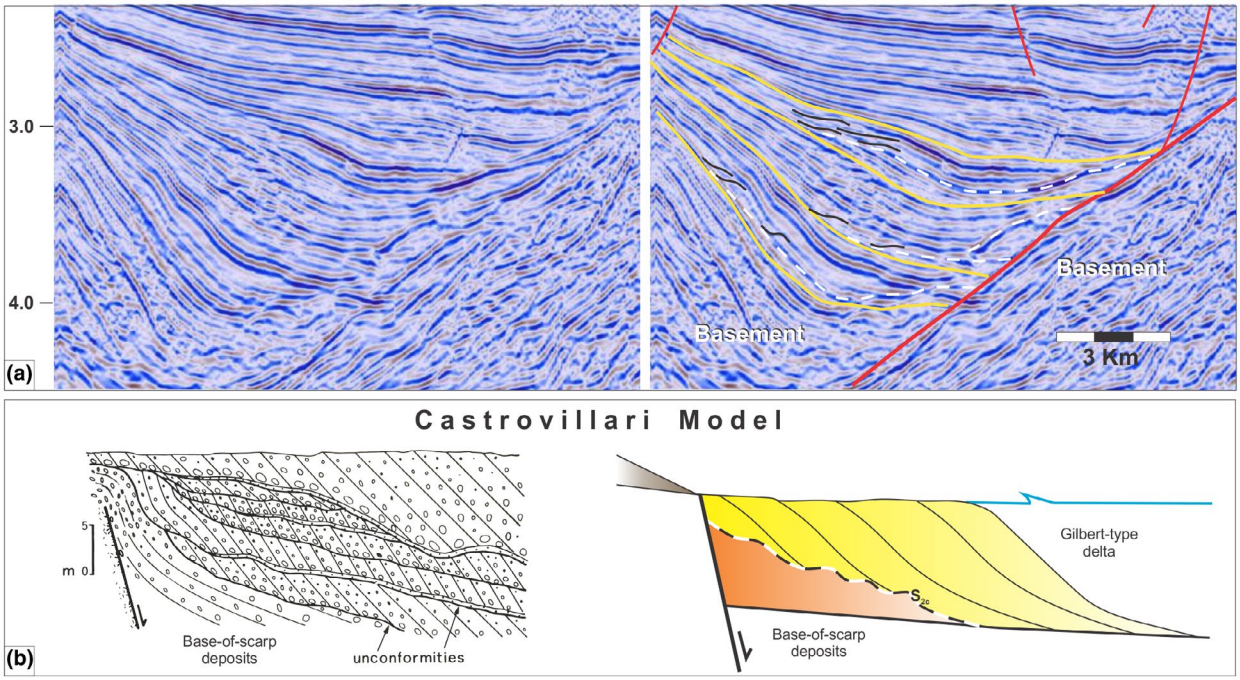

FIGURE 1 Subsurface and outcrop examples of fault-controlled systems developing a base-of-slope alike deposits on which Gilbert-type systems develops. (a) Vertically stacked units of the Bohai Bay (China) extensional system producing unsteady wedge-shaped deposits evolving to steady-state Gilbert systems. The Gilbert systems develop above an unconformity surface (dashed line; modified from Jia et al., 2019). (b) The Castrovillari Model proposed by Colella (1988b) for the vertically stacked systems recognised in the Crati Basin (Italy). Accumulation assimilable to the proposed base-of-scarp deposits is reported during the early stage. Important to highlight as in both cases, the interpreted base-of-scarp deposits are capped by an unconformity surface (S_2) separating the unsteady and steady-state systems

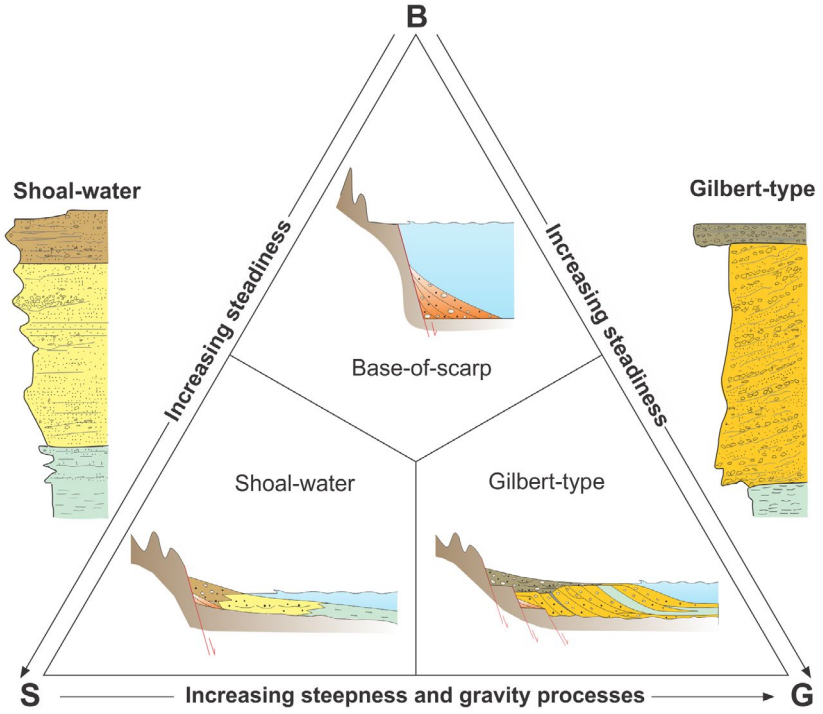

FIGURE 2 BSG schematic diagram of fault-controlled systems (not in scale). Base-of-scarp deposits (B) represents the unsteady-state end-member. The shoal-water (S) and Gilbert-type (G) represent the steady-state of fault-controlled systems for which two representative vertical sequences are shown (See Figure 5 for the base-of-scarp typical vertical sequence). Mixed systems can exist in the triangle depending on the interaction between sedimentary supply rate and accommodation. Transition to Gilbert-type or shoal-water systems controlled by the steepness of the subacqueous slope and depostional processes fully dominated by sediment gravity-transport processes for the Gilbert-type. Embryonic base-of scarp deposits are indicated in orange in all three end-members

the lower portion of the Early-Middle Pleistocene Civita section (Figure 4a). The Civita section developed in the northern sector of the Crati Basin along a fault-segment of the 15-km long Pollino Fault (Colella, 1988a,b; Filice and Seeber, 2019), and pertain to the Pleistocene Synthem (PlS) defined by Spina, Tondi, and Mazzoli (2011; Figure 4a). The Pollino Fault has an oblique normal-sinistral kinematics (Chiarabba, Agostinetti, & Bianchi, 2016; Ghisetti & Vezzani, 1982; Monaco & Tansi, 1992; Tansi et al., 2007, 2016; Van Dijk et al., 2000) forming a SW facing fault scarp that favoured the formation of several vertically stacked Plio–Pleistocene deltaic units having a total thickness of ~300 m (Colella, 1988b; Figure 4a). Depositional architectures indicate a dominant southwest evolution of the system (Colella, 1988a). Towards the south, the Early-Middle Pleistocene deposits are overlain by Middle-Upper Pleistocene lacustrine sediments (Colella, 1988a; Spina et al., 2011). Along the Raganello Stream (Figure 5), the Early-Middle Pleistocene coarse-grained deposits are locally overturned, and unconformably overlain by Late Pleistocene–Holocene fluvial terrace deposits (Figure 4a). Overturned strata are related to transpressional jogs and bends along the Pollino fault zone (Catalano, Monaco, & Tansi, 1993; Ferranti, Santoro, Mazzella, Monaco, & Morelli, 2009) active after the deposition of the Early-Middle Pleistocene coarse-grained deposits of the Civita section. The Civita section has been previously interpreted as a stacked Gilbert delta succession referred to as the Castrovillari model (Colella, 1988a)—a Gilbert-type delta succession recording several episodes of tectonic activity in the form of erosive, bounding sequences separated by unconformities related to the activity of basin bounding normal faults. However, the lower portion of the Civita section shows neither a bottomset nor a topset but only inclined beds forming a wedge-shaped body characterised by an upward decrease in strata dip, thinning towards and onlapping against the fault scarp (Figure 6a–c).

3.1.2 | The Messina strait

The Messina Strait developed during a Pliocene phase of structurally controlled narrowing, related to the tectonic activity of an NNE-SSW-oriented faults system known as 'Siculo-Calabrian Rift Zone' (SCRZ) which dissects the Palaeozoic metamorphic rocks of the Peloritani-Aspromonte Massifs and controlled the evolution and accumulation of deposits were peformed along the basin margins through a synsedimentary activity (Catalano, De Guidi, Monaco,

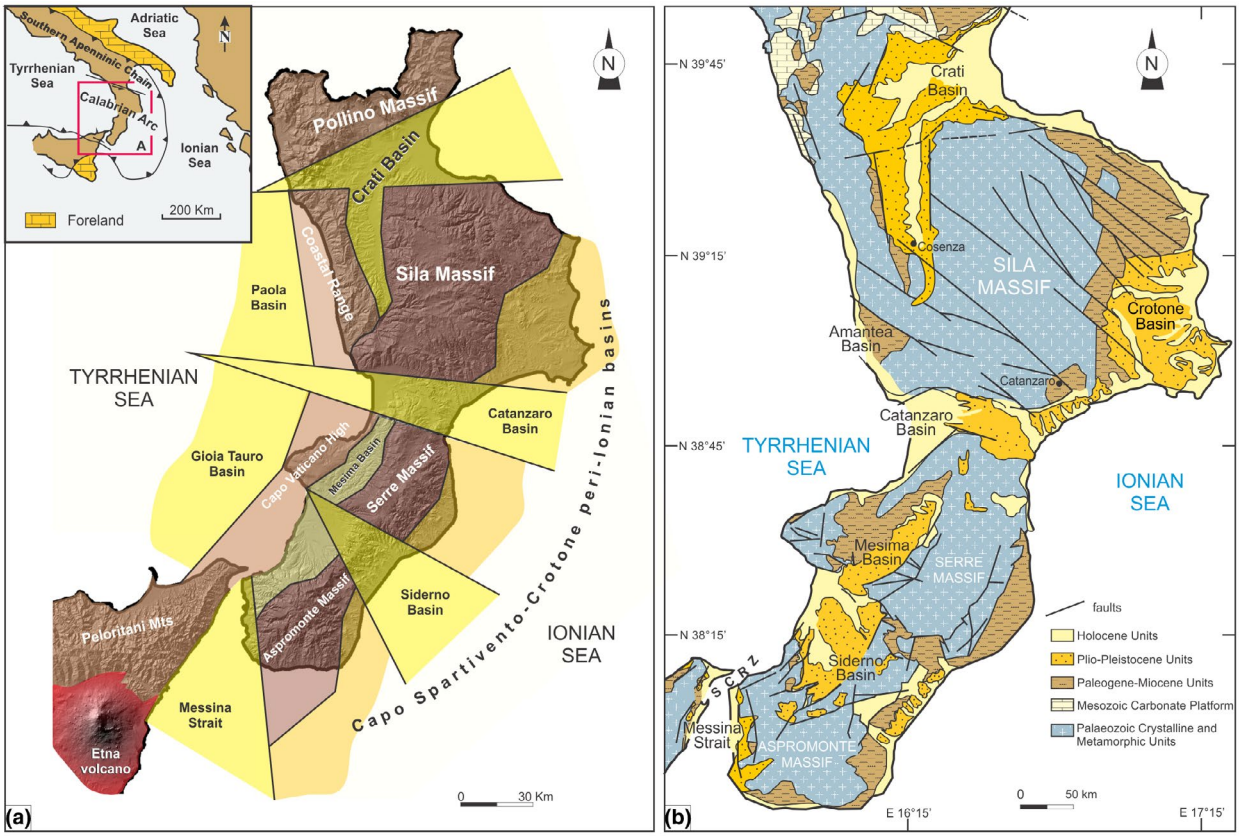

FIGURE 3 (a) Plio–Pleistocene block-segmentation of the Calabrian Arc in southern Italy (insert) within the resulting yellow sedimentary basins (Chiarella, 2016 redrawn after Ghisetti, 1979). (b) Simplified geological map of the Calabrian Arc (modified after Longhitano et al., 2012). SCRZ: Siculo-Calabrian Rift Zone

Tortorici, & Tortorici, 2008; Ghisetti, 1984, 1992; Monaco & Tortorici, 2000; Monaco, Tortorici, Nicolich, Cernobori, & Costa, 1996; Tripodi, Muto, Brutto, Perri, & Critelli, 2018; Figures 3b, 4b and 7). The studied Messina Strait examples comprise fault-controlled deposits of the Croce Valanidi and San Teodoro sections located on the eastern margin of the strait along the Armo normal fault (Figures 4b, 6d,e and 7). The Armo Fault is a ~12-km long NNE-SSW-striking, NW-facing breached monocline controlled the location of depocentres and the abrupt along-strike thickness, and facies change of the Pleistocene deposits. On the Armo Fault, the Pliocene to present fault throw is ~350 m with a time-averaged throw rate of $0.7 + 0.3/-0.2$ mm a^{-1} based on terrace offsets (Ghisetti, 1992; Roda-Boluda & Whittaker, 2017). During the initial extensional phases, the Armo Fault was blind producing a basinward-facing monocline (extensional forced fold), which controlled the deposition of the early Plio–Pleistocene marginal deposits of the Vinco Calcarenites Unit (Ghisetti, 1992)—deposits that despite the name actually consists of a compositional mixing of bioclastic and siliciclastic sediments (sensu Chiarella, Longhitano, & Tropeano, 2017; Figure 8). The Vinco Calcarenites were deposited in stratigraphic wedges that thin towards and onlap onto the growth fold and are topped by middle Pleistocene deltaic deposits of the Messina Gravels and Sands Formation (Figure 4b). The identification of the boundary between the Vinco Calcarenites Unit and the Messina Gravels and Sands Fm is facilitated in the field by the mixed bioclastic–siliciclastic nature of the Vinco Calcarenites. Mixed composition representing a distinctive feature of many Plio–Pleistocene deposits accumulated in the Mediterranean area (e.g. Chiarella, Longhitano, Sabato, & Tropeano, 2012; Longhitano et al., 2012; Longhitano, Chiarella, & Muto, 2014; Massari & Chiocci, 2006; Nalin, Ghinassi, Foresi, & Dallanave, 2016; Pepe & Gallicchio, 2013; Rossi et al., 2017; Yesares-García & Aguirre, 2004), and would reflect specific conditions of sediment deposition very sensitive for recording local hydrodynamics processes (Chiarella & Longhitano, 2012; Chiarella, Longhitano, & Tropeano, 2019). The lower and proximal portion of the Vinco Calcarenites have been referred in the literature as intraformational breccias and mass-wasting deposits associated with subaqueous steep cliffs (Longhitano, 2018 and references therein). Upwards, the system evolves to shallower deposits of the same Unit (Figures 4b and 6e).

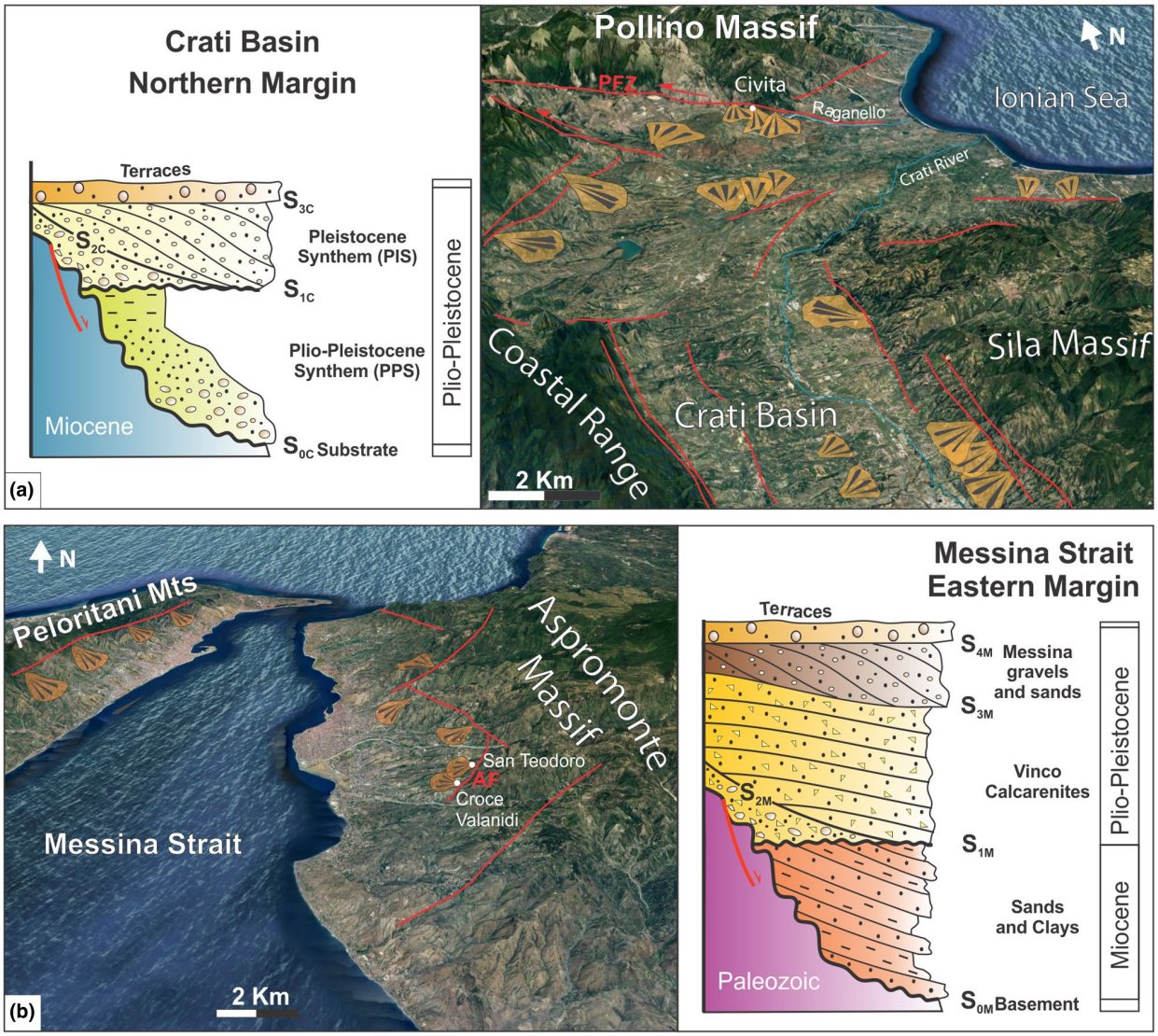

FIGURE 4 (a) Schematic stratigraphic column of the northern margin of the Crati Basin, and map showing the distribution of fault-controlled Plio–Pleistocene systems in the eastern and northern portion of the Crati Basin. (b) Schematic stratigraphic column and map showing the distribution of fault-controlled Plio–Pleistocene systems in the eastern margin of the Messina Strait. PFZ: Pollino Fault Zone. AF: Armo Fault. Small-scale distortion from the base to the top of the satellite images to be considered

4 | METHODOLOGY

To investigate the unsteady-state base-of-scarp deposits and their evolution to steady states, the following methods are used: large- to small-scale outcrop observations followed by conventional sedimentological analysis; and line-drawing performed on panoramic photos to investigate the proximal to distal variation of bedding attitude and geometry. We specifically selected outcrops to characterise the key depositional elements and detect variations in facies along strike and dip. Field observations have been combined to form a representative vertical sedimentary succession of the base-of-scarp deposits (Figure 9).

The studied units are easily distinguishable and laterally observable, thanks to a good degree of exposure common to both study areas. Moreover, studied units have been locally documented in several previous outcrop-based studies (e.g. Barrier, 1986; Colella, 1988b; Ghisetti, 1992; Longhitano, 2018; Roda-Boluda & Whittaker, 2017).

Finally, the concept of depth-ratio (*cfr*. Jopling, 1965) has been used to characterise the relationship between the water depth at the footwall crest and the basin water depth of the hanging wall. Accordingly, a low depth-ratio means a high difference in water depth between the footwall crest and the hanging wall, and a high depth-ratio means a small depth difference.

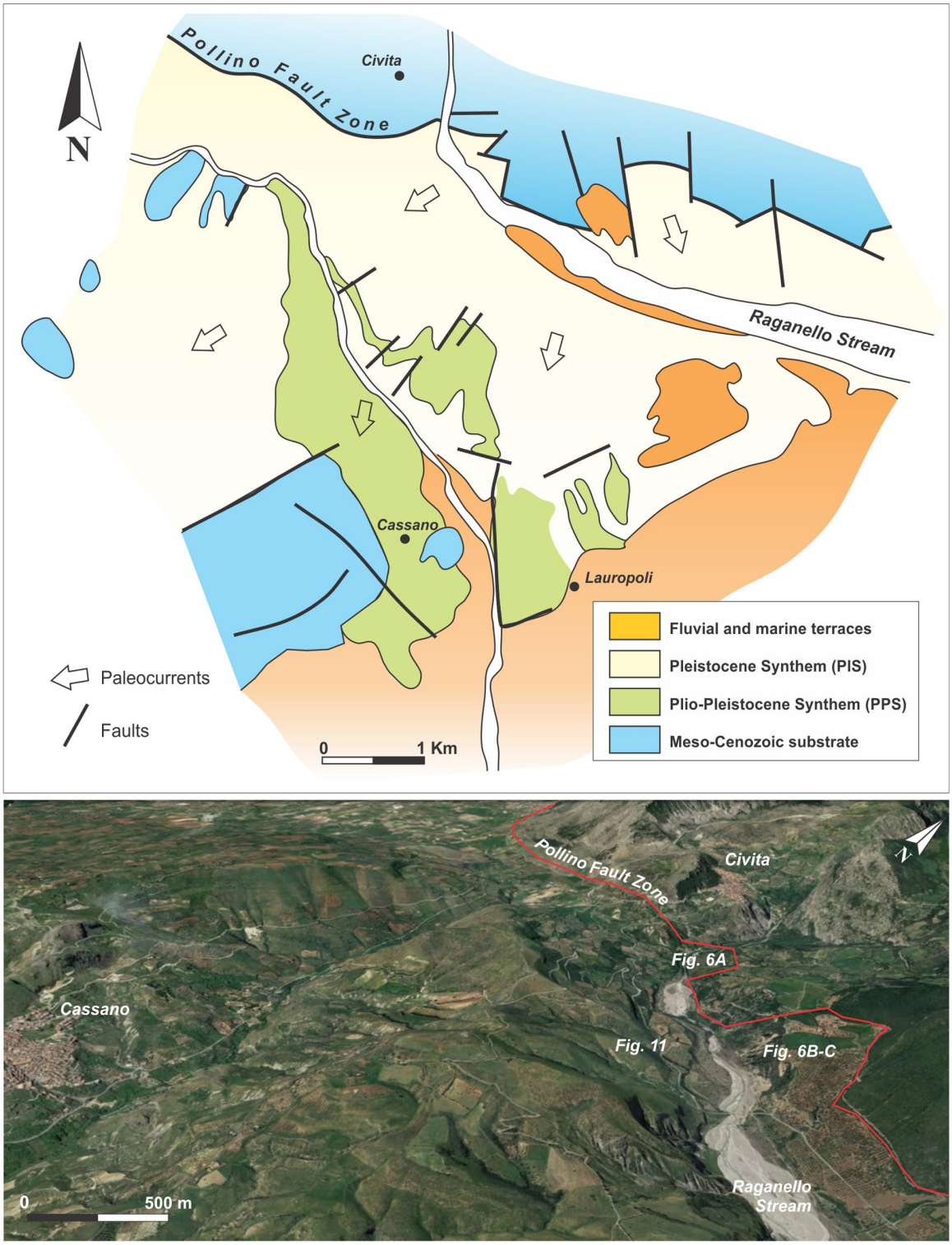

FIGURE 5 Geological sketch map of the Pollino Fault Zone (Crati Basin) showing the main deposits and tectonic elements. The Pollino Fault was active during the sedimentation of the Plio–Pleistocene Synthem (PPS) controlling the evolution of the deposits. Arrows indicate the main progradation direction of the Plio–Pleistocene units. The panoramic view illustrates the position and relative geographic position of the studied outcrops and the controlling fault within the system

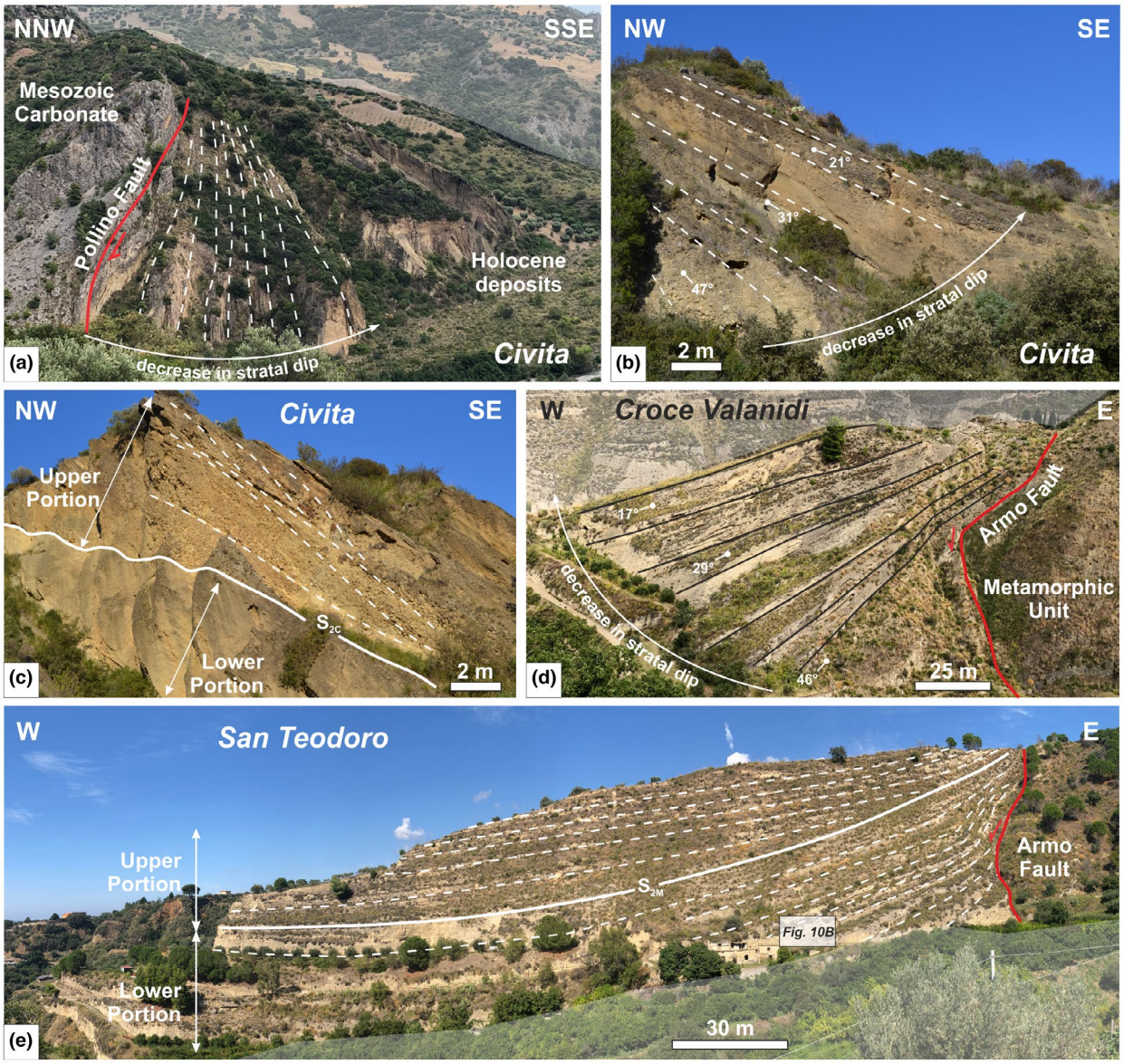

FIGURE 6 Fault-perpendicular wedge-shaped architectures of base-of-scarp systems characterised by a general upward decrease in the strata dip suggesting basinward expansion of the early syn-rift successions. (a-c) Panoramic views of the Civita section along the Raganello Stream (see Figure 5) showing the contact of the deposits of the lower portion over the Carbonate units of the substrate (a) and the upward transition between deposits of the lower portion to the Gilbert-type system of the upper portion (c). Panoramic views of the Croce Valanidi (d) and the San Teodoro (e) sections (see Figure 7) showing the relationship with the underlying metamorphic basement unit and the upward transition between the lower portion and the shoal-water system of the upper portion (e). This transition is marked by the presence of an angular unconformity (S_2)and a change in strata geometries

5 | ANATOMY OF BASE-OF-SCARP DEPOSITS

5.1 | Civita section (Crati Basin)

5.1.1 | Stratal architecture and facies

Early-Middle Pleistocene coarse-grained deposits of the Civita section unconformably overlie Mesozoic carbonates along the scarp of the Pollino Fault (Figures 4a and 5). The lower portion of the Civita section shows a wedge-shaped geometry characterised by a gradual upward decrease in strata dip within the unit (Figure 6a,b). In particular, a difference of ~25° is appreciable between the lower and the upper strata suggesting a southward thickening of the unit. Sediments derive mainly from the Meso-Cenozoic carbonate and flysch units representing the substrate of the fault-controlled basin margin.

In the proximal and lowermost portion of the system (Figures 5 and 6a,b), next to the fault scarp, strata consist of

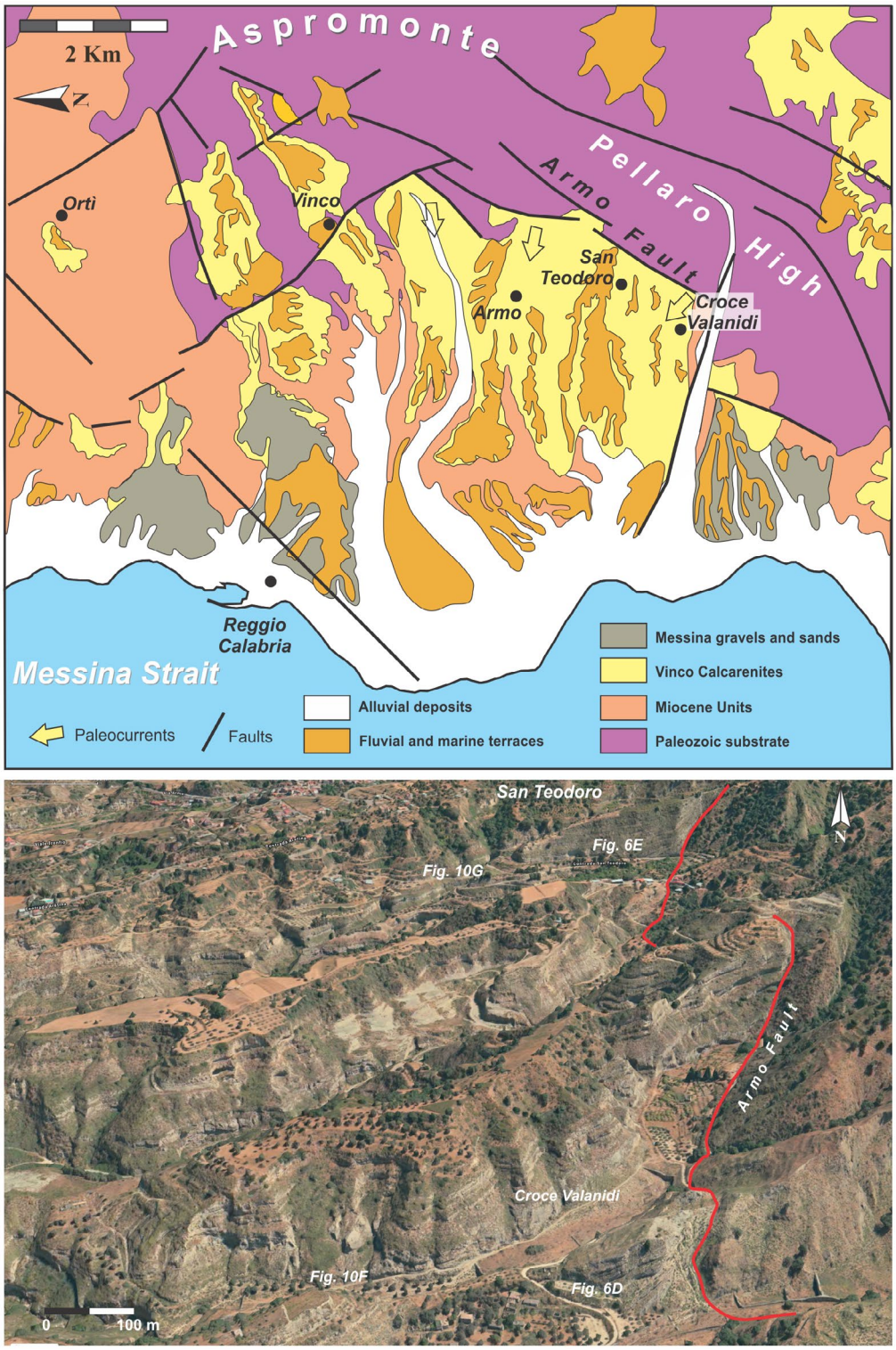

FIGURE 7 Geological sketch map of the Armo Fault area (Messina Strait) showing the main deposits and tectonic elements. The Armo Fault was active during the sedimentation of the Vinco Calcarenites unit controlling the evolution of the deposits. Arrows indicate the main progradation direction of the fault-controlled Vinco Calcarenite Unit. The panoramic view illustrates the position and relative geographic position of the studied outcrops and the controlling fault within the system. The San Teodoro and Croce Valanidi sections develop along the same fault and are ~1 km apart

gravel-to pebble-sized breccias supported by a fine-to medium-grained sand (Facies 1; see Figure 10a from the Messina Strait section as example). Moving upwards, strata become more organised showing an alternation of conglomerate and sandstone beds (Facies 2; Figure 10c,d), with the sandstone portion becoming progressively dominant (Figure 10e). Gravel beds are up to 50 cm thick and consist of poorly to moderately sorted, matrix- to clast-supported, sub-rounded to

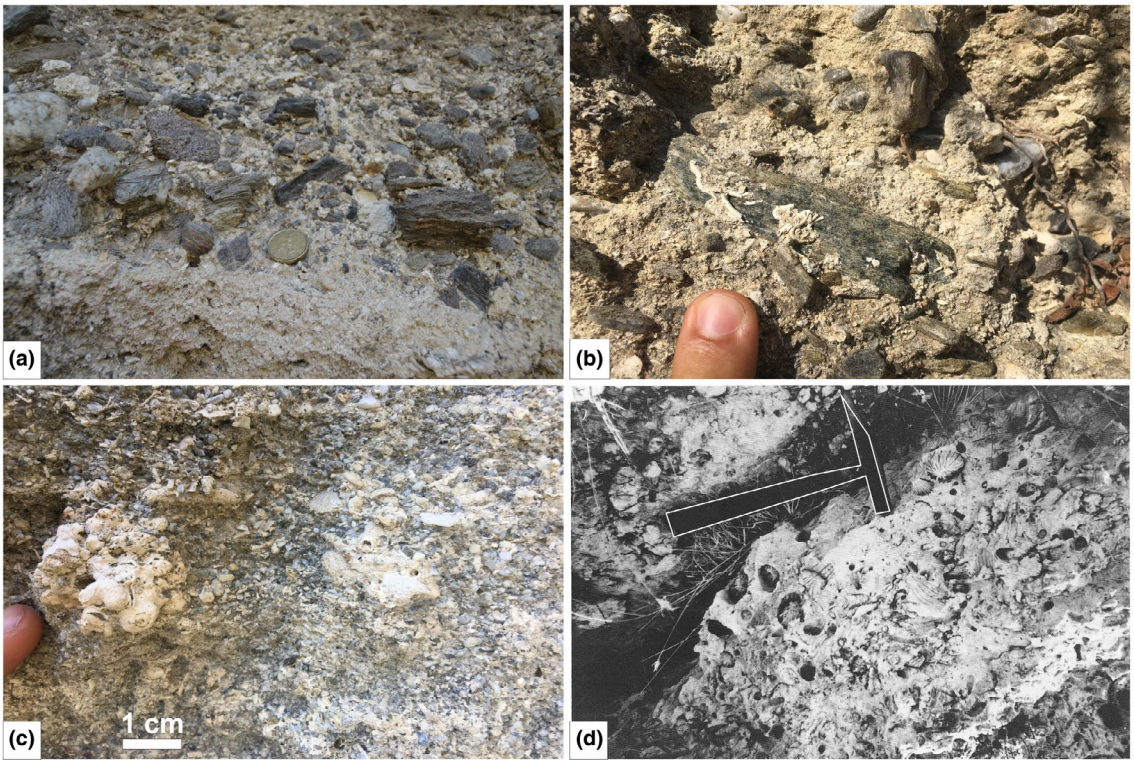

FIGURE 8 Close-up view of the Vinco Calcarenite mixed siliciclastic-carbonate deposits forming a compositonal mixing (sensu Chiarella et al., 2017). (a) Mixture of poorly sorted angular metamorphic gravels and bioclastic sandstone. (b) Elongated metamorphic clast enclosed within a bioclastic matrix and encrusted by serpulids. (c) Cool-water carbonate sediments composed of bryozoans fragments mixed with a siliciclastic fraction. (d) Bathyal *Desmophyllum cristagalli, Isis sp* corals along the Armo Fault (from Barrier et al., 1986)

rounded pebbles and cobble conglomerates. Matrix is sand-gravel grade, and locally clasts are imbricated. The sandstone beds include coarse-grained, moderately to poorly sorted, sub-angular to sub-rounded arenite. Locally, scattered granules and pebbles occur. Unfortunately, the vertical attitude of the strata does not allow to properly evaluate the proximal to distal variation of the facies with respect to the fault scarp or to infer with the primary depositional dip angle of the palaeo-slope.

At the top of the lower portion (~100 m above the basal contact), an angular unconformity (S_{2C}), locally draped by a ~50 cm thick interval is made of a matrix-supported conglomeratic layer passing upwards to silt and fine-grained sand present as solitary bed, separates the wedge-shaped deposits from an upper portion characterised by prograding foreset elements (Figure 11). Foresets downlap above the angular unconformity, or the corresponding relative drape, (Figures 6c and 11) and are part of the younger steady-state Gilbert-type delta pertaining to the Castrovillari model defined by Colella (1988b).

Depositional processes are suggested to have been dominated by sediment gravity flows (Colella, 1988b), such as gravel-rich inertial grain flows to non-cohesive debris flows, and high-density turbidity currents (Nemec, 1990).

The presence of an angular unconformity (S_{0C}, Figure 4a) between the Mesozoic carbonates and the lowermost syn-rift deposits of the Civita section along the Pollino Fault (Figure 5) suggests that a pronounced relief was associated with this structure at the onset of syn-rift deposition. Based on the gradual change of the dip angle between the lower and the upper strata of the lower portion, we suggest that the Pollino Fault was active during the sedimentation controlling the accumulation of the wedge-shaped deposits of the Civita section as indicated by the presence of the intraformational unconformity S_{2C}. Accordingly, these deposits were accumulated in a syn-rift wedge that thinned towards the Pollino Fault (Figure 6a,b).

The different sedimentation style above the unconformity S_{2C} follows the shutdown of the deposition of the lower portion and suggests a rapid change in basin conditions, and potentially relative water depth, probably related to the activity of the controlling fault. The result is a change in the depositional profile producing a depositional angle suitable for the development of a Gilbert system. In fact, the S_{2C} unconformity separates the unsteady deposits from the steady-state Gilbert-type delta. Important to highlight is that the distinctive character of the Castrovillari model defined by Colella (1988b) is the recognition of vertically

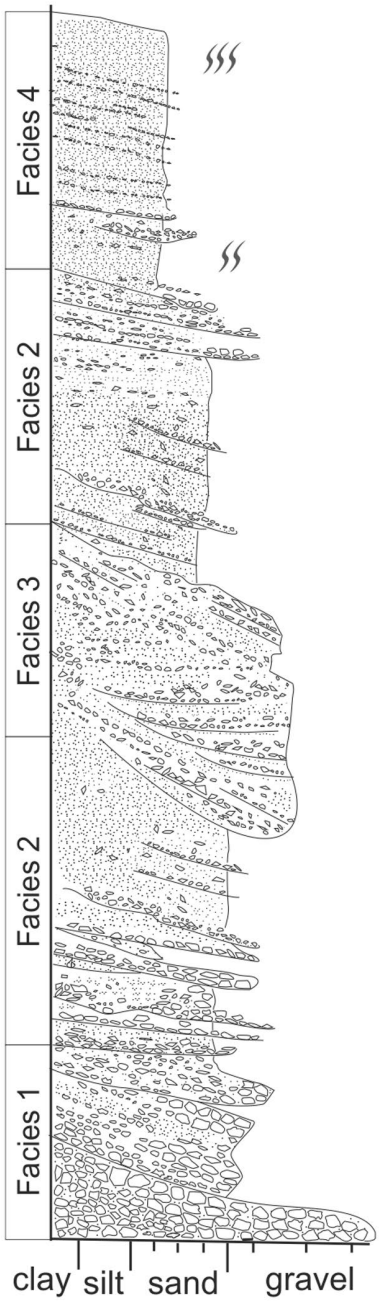

FIGURE 9 Representative sedimentological log for base-of-scarp deposits showing a fining-upward general trend. The base of the system is composed of a breccia passing upward to conglomerates and sands organised in tabular beds locally characterised by the presence of backsets. The succession therefore shows channelised depositional elements infilled by conglomerates and sands. Distally, the system pass to more sandy deposits (although it is still possible to recognise conglomeratic event beds) evolving into bioturbated sandy beds

stacked units separated by major irregular surfaces related to slides resulted from high-magnitude fault slip events (Colella, 1988b).

5.2 | Croce Valanidi and San Teodoro sections (Messina Strait)

5.2.1 | Stratal architecture and facies

The Plio–Pleistocene syn-rift Vinco Calcarenites Unit of the Croce Valanidi and San Teodoro sections lies nonconformably on top of Palaeozoic metamorphic rocks of the Peloritani-Aspromonte Massifs along the Armo Fault, and through an angular unconformity on top of Miocene deposits in the distal area. The nonconformable surface represents the base syn-rift unconformity S_{0M} (Figure 4b). Depositional architectures and elements (e.g. channels) indicate a west-northwest evolution of the system, almost perpendicular to the present-day orientation of the Messina Strait (Figure 7).

The studied deposits at the Croce Valanidi and San Teodoro sections are characterised by a wedge-shaped geometry exhibiting a gradual upward decrease in strata dip (Figure 6d,e). At the Croce Valanidi section, the system shows a difference of ~30° in the dip between the lower and the upper strata. This geometrical relationship becomes less pronounced in the upwards portion of the succession where layers are almost sub-horizontal (Figure 6e). The deposits consist of a siliciclastic fraction mainly represented by metamorphic clasts mixed with a carbonate bioclastic component (Figure 8a). Clasts encrusted by serpulids have been observed (Figure 8b). The bioclastic fraction contains a mixture of cool-water carbonate factory (e.g. bryozoan, brachiopods, echinoids; Figure 8c) and bathyal corals (e.g. *Madrepora oculata, Lophelia pertusa, Desmophyllum cristagalli, Isis sp.*; Barrier, 1986; Barrier, Di Geronimo, & Lanzafame, 1986; Figure 8d).

The most proximal and basal deposits recognised in the lower portion next to the Armo Fault (Figure 6d,e) are characterised by immature gravel- to pebble-sized breccia and poorly sorted conglomerate clasts mixed with coarse-grained bioclastic fragments to form a 20- to 200-cm thick interval (Facies 1). Upwards, beds are typically composed of coarse-grained bioclastic–siliciclastic sand and conglomerate gravel (Facies 2). In a proximal position (~60 m away from the fault scarp), Facies 2 beds form packages consisting of structureless coarse-grained sandstone with clustered or scattered angular gravel clasts and non-graded or coarse-tail inversely graded matrix- to clast-supported conglomerate (Figure 10a). Locally, these packages are separated by 50- to 200-cm thick layers of amalgamated sandstone with non-erosional bases (Figure 10b). Here the inclined bed succession includes also isolated, downdip trending scours up to ~60 cm deep, filled with sandy and gravelly cross-strata dipping upslope at up 30 degree relative to general bedding (Figures 6b and 12). Three hundred meters away from the scarp, conformable

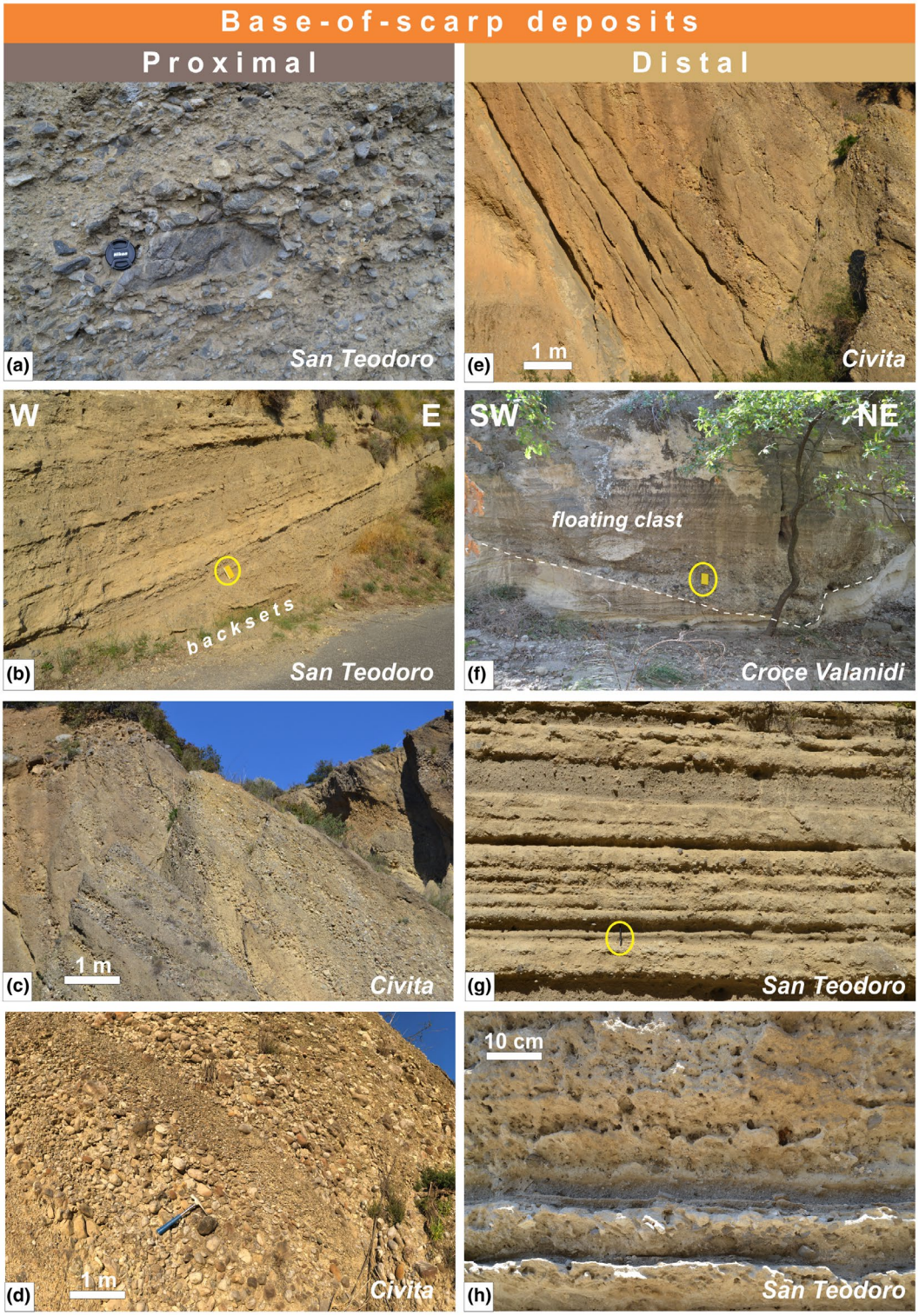

FIGURE 10 Overview of sedimentary facies in proximal (~50 m away from the fault scarp) and distal positions (300–450m away from the fault scarp) positions from both Crati Basin and Messina Strait (see Figures 5 and 7 for outcrops relative distance). Facies 1: (a) Non-graded pebbly sandstone with lenticular intervals of breccia and clast-supported conglomerate showing a coarse-tail inversely grade trend. Facies 2: (b–d) Tabular alternation of clast-supported conglomerates and sandstone beds at the San Teodoro (b) and Civita (c,d) sections. Upslope migrating chute-fill backsets characterise the lower part of the insert B (see Figure 12). (c) Close-up view of the conglomeratic-sandstone alternation. (e) In the distal portion of the system, stratified medium- to coarse-grained sandstones dominate Facies 2. Facies 3: (f) Conglomeratic channel with large floating clast in the upper part cutting through, and covered by, tabular sandstones. Facies 4: (g) Tabular fine- to medium-grained sandstones with isolated clasts; (h) Bioturbated intervals (*Thalassinoides*)

FIGURE 11 Stratigraphic transition between the unsteady- base-of-scarp deposits and the steady-state Gilbert-type delta in the Civita section (Crati Basin). The transition is marked by the S_{2C} unconformity topped by a thin compound interval made up of gravel evolving to fine-grained sand and siltstone

beds of Facies 2 are interrupted by discontinuous, massive to coarse tail inversely graded conglomerate-sandstone packages (Facies 3). This deposit results in channelised features (10–50 m wide, 2–5 m thick) forming 2- to 3-m thick event beds containing isolated large outsized floating clasts (up to 100 cm in size; Figure 10f). In the distal position (~450 m away from the fault scarp), deposits consist of structureless to stratified, fine- to medium-grained sandstone with floating subangular to subrounded pebbles (Facies 4; Figure 10g). Intensely bioturbated intervals separate the structureless and laminated sandstones (Figure 10h).

The sedimentary facies are all indicative of gravity-driven sediment-transport events, such as high-density turbidity currents, debris flows and debris falls. Upslope-dipping cross-strata represent backsets related to supercritical flows (Nemec, 1990; Massari, 1996; Ono & Plink-björklund, 2018; Postma et al., (in press)). Outsized clasts may be emplaced by bipartite flows including basal dense flow and upper bypassing turbidity current (Postma, Nemec, & Kleinspehn, 1988) or by debris falls (Nemec, 1990). The presence of encrusted metamorphic clasts suggests that the siliciclastic fraction derives from an intrabasinal submarine sediments source like the exposed fault scarp, or from the footwall area through shallow-marine deltaic systems. Additional clastic sediment contribution can directly be sourced from onshore during episodic river-generated catastrophic flash flood as documented in southern Italy (Sorriso-Valvo & Terranova, 2006). The carbonate fraction results from the fragmentation of coeval in situ or near situ carbonate factories developed along the footwall crest and at the base of the scarp. Based on the recognised bathyal species, Barrier (1986) estimates a water depth ≥600 m for the deposits of the studied sections.

The unconformity S_{2M} separating the lower from the upper portion of the Vinco Calcarenites Unit marks an abrupt change in the depositional architecture: from underlying fault-controlled wedge to overlying tabular deposits related to a quiescent phase (Figure 6e). The upper portion gently laps against either the lower portion or directly on the metamorphic substrate of the footwall (Figure 6e). Moreover, the upper portion contains wave-influenced sedimentary structures and lack of bathyal corals in the proximal area passing distally to current-dominated, tide-influenced cross-strata migrating parallel to the palaeomargin and related to the ancient Messina Strait suggesting the evolution to a shoal-type system characterised by reworking in its distal environments. For a detailed documentation of the sedimentological facies recognised in the upper and distal portion of the Vinco Calcarenites unit, the reader is referred to Longhitano (2018).

The presence of an extensive unconformity between the pre-rift (i.e. Peloritani-Aspromonte Unit and Miocene deposits) and the lowermost syn-rift deposits along the Armo Fault suggests that the Armo Fault was already active during the deposition of the Vinco Calcarenites Unit. We interpret that the growing geometry producing the landwards thinning towards the Armo Fault recognised at the Croce Valanidi and San Teodoro sections is related to the initiation of forced folding above this structure during the early syn-rift stage. The absence of deposits along the footwall can be both due to non-deposition (i.e. bypass) or erosion. Important to highlight is that the area has been subject to a time-averaged throw rate quantified using terraces elevation of $0.7 + 0.3/-0.2$ mm a^{-1} (Ghisetti & Vezzani, 1982; Roda-Boluda & Whittaker, 2017) producing a fault throw of ~350 m, quantified using terraces elevation, favouring the exposure and/or remobilisation of footwall deposits.

The overall shallowing upward transition between the lower and the upper portion marks the change in the depositional architecture between the unsteady wedge-shaped deposits and the steady-state shoal-water deposits suggesting that sediment-supply rate exceeded the fault-slip rate.

FIGURE 12 Close-up view (top) and line drawing (bottom) of chute-fill backsets located along the slope (San Teodoro section, Messina Strait). The scour is produced by an episode of supercritical flow and filled in by subcritical flows due to hydraulic jump. The main depositional flow moved towards the left of the photo with the source area located on the right. See Figure 10b for the location

6 | DISCUSSION

The lower portion of the studied sections (a) is controlled by an active fault, (b) evolves from an unsteady to a steady state (e.g. Gilbert- or shoal-type deltas; (c) lacks sedimentary structures related to wave action and lateral equivalents typical of coastal marine or terrestrial facies, (d) accumulated in a subaqueous setting below the storm-base as a body detached from a subaerial counterpart, (e) contains bathyal corals suggesting that they have been deposited in a relatively deep-water setting and (f) is characterised by an extremely low depth-ratio (sensu Jopling, 1965) defined as the ratio

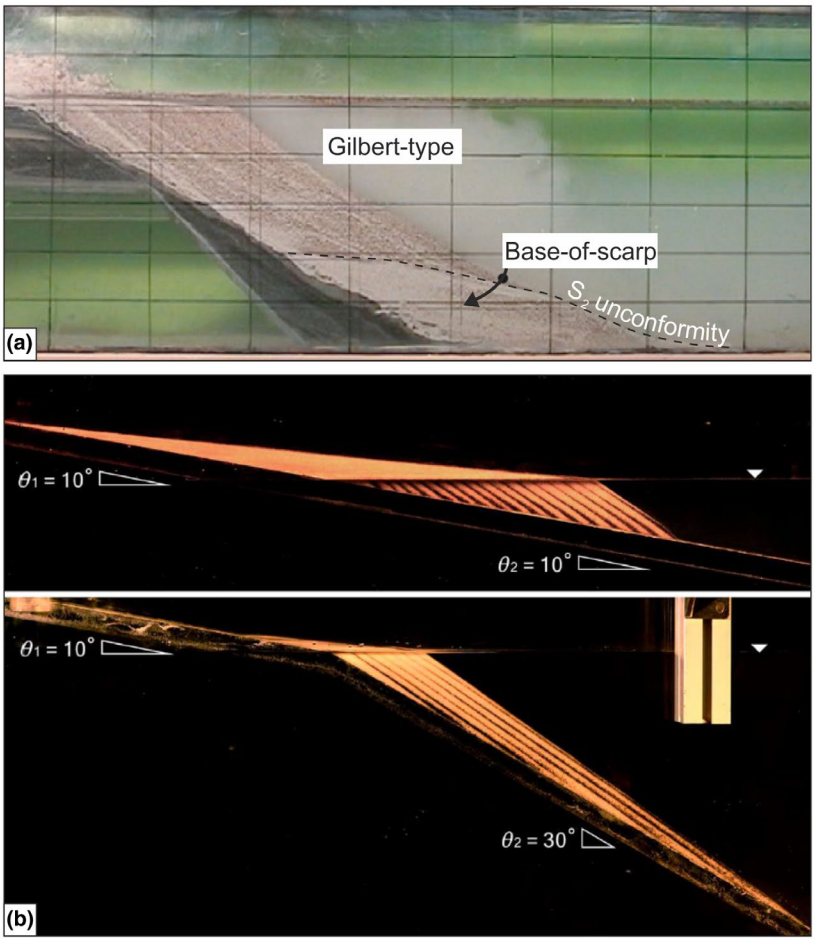

FIGURE 13 (a) Flume experiment showing the accumulation of what here is defined base-of-scarp deposits during the early depositional phases. The base-of-scarp deposits subsequently evolve to a Gilbert-type delta system prograding above an unconformity separating the unsteady to the steady-state phases (modified after Abeyta & Paola, 2015). The unconformity can be referred to as the S_2 surface recognised in the studied examples. (b) Profile of Gilbert-type deltas evolving above depositional surface characterised by different depositional angles (modified after Lai et al., 2017)

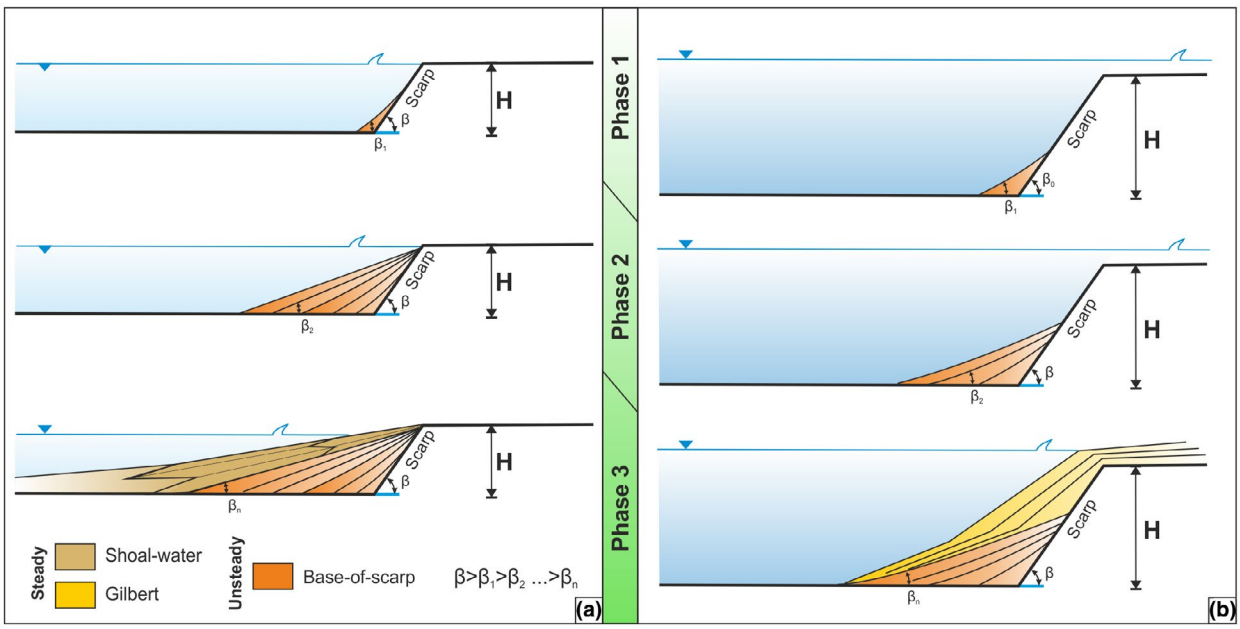

FIGURE 14 Schematic representation of unsteady-state base-of-scarp system evolving into (a) shoal-water and (b) Gilbert-type systems characterised by a steady-state condition. The progressive angle decrease recognised in the younger strata promotes the architectural change of the system. 'ß' indicates the starting, intermediate ($\beta_{1,2...}$) and final (β_n) depositional angle of the unsteady-state deposits, while 'H' the throw. The scarp represents the bypass area produced by either by a forced fold or a fault plane. Inspired after Nemec (1990)

between the water depth at footwall edge and the water depth at the hanging wall (i.e. base of the scarp). Given this setting and the predominance of texturally immature sediment gravity flow deposits, we infer that sediments were transferred through a proximal sediment bypass zone (sensu Stevenson, Jackson, Hodgson, Hubbard, & Eggenhuisen, 2016) and experienced a very limited rework and transport before being accumulated. These distinctive characters thus suggest that they differ from 'classical' fault-controlled deposits (e.g. Gilbert- and shoal-water-type deltas; Massari & Colella, 1988) typically characterised by a steady-state evolution with systems growing in size without altering their shape, shallow-marine environments and high depth-ratio. For this reason, this class of deposits are termed 'base-of-scarp' here to highlight the importance of an embryonic unsteady-phase at the base of fault-controlled systems.

6.1 | Relationship between fault slip, sedimentation and internal geometry

Even though in the literature the Civita section has been considered at basin-scale to be part of a vertically stacked Gilbert-type deltas (Colella, 1988a), we interpret that the lower portion of the system represents a separate base-of-scarp system onlapping against the controlling fault scarp without developing topset facies. In the Crati Basin example, the Pollino Fault controlled the development of the Civita section. An increase of the fault-slip rate exceeding the sediment-supply rate may have created the conditions to evolve from an unsteady base-of-scarp ('B' vertex of the BGS triangle; Figure 2) to a steady-state Gilbert-type system ('G' vertex of the BGS triangle; Figure 2) through the remobilisation of large portions of sediment and re-definition of the depositional profile favourable for the development of a steady-state system. The boundary between the two end-members (i.e. base-of-scarp versus. Gilbert type) is highlighted by the unconformity surface S_{2C} (Figures 4a, 6c and 11). Unconformity surfaces that were already interpreted by Colella (1988b) in the Civita section as surfaces and interpreted as surfaces related to gravitational sliding of coarse-grained material linked to tectonic vertical displacement (Figure 1b). Fault activity responsible also for the re-adjustment of the depositional profile towards a less inclined slope profile necessary for the development of a Gilbert-type system (Figures 13a and 14).

The stratigraphic vertical evolution recognised in the Croce Valanidi and San Teodoro sections (Figure 6e) shows wedge-shaped deposits passing upwards to sub-horizontal, finer-grained beds. This trend indicates that the base-of-scarp system gradually reduced from the base to the top of the dip angle of the depositional profile (Figure 6d,e). Moreover, the fining-upward trend recognised in the base-of-scarp systems (Figure 9) differs markedly from the progradational coarsening-upward trend commonly suggested for deltaic successions (Miall, 1976) and alluvial fans (Steel, Moehle, Nilson, Roe, & Spinnangre, 1977), and is typical rather of colluvial systems (Blikra & Nemec, 1998; Longhitano, Sabato, Tropeano, Murru, & Carannante, 2015; Nemec, 1990). The upwards transition from inclined to subhorizontal beds indicates that the lower portion of the Croce Valanidi and San Teodoro systems corresponds to a base-of-scarp deposit ('B' vertex of the BGS triangle; Figure 2), whereas the upper portion represents a transition to a tide-influenced and current-dominated shoal-water system corresponding to the 'S' vertex of the BGS triangle (Figures 2 and 6e). This transition suggests that the upper portion developed in a more stable and shallower setting when the controlling fault reduced its activity or became inactive. Conversely, the lower portion is characterised by a wedge-shaped geometry highlighted by the gradual upward decrease in strata dip, and strata thickening away from the fault (Figure 6d,e). This suggests that the controlling fault was active during the deposition of the lower portion producing a monocline, subsequently breached, where strata onlap it. The Croce Valanidi section occurs ~1 km southwest along the Armo Fault (Figure 7), with respect to the San Teodoro section. The different behaviour of the San Teodoro and Croce Valanidi systems might reflect differential fault displacement along the fault scarp (fault tip versus. centre) leading to different subsidence and fault-activity patterns (e.g. Barrett et al., 2019), or diachronous onset of the folding along strike (Lewis et al., 2015).

The development of unsteady base-of-slope deposits versus steady-state systems (e.g. Gilbert-type or shoal-water-type systems) seems to be mainly controlled by (a) the angle of the depositional slope above which sediments accumulated, (b) fault activity, (c) depth-ratio and (iv) the ratio between the fault scarp displacement and the rate of sediment supply.

(a) Experimental studies based on flume reconstructions (e.g. Lai, Hsiao, & Wu, 2017) show that in order to initiate the development of Gilbert-type deltas, the angle of the basal depositional slope typically must correspond to a range comprised between 30 and 10 degrees (Figure 13b), where the exact value depends from different aspects including sediment sorting, grain-size and particle shape and grain-size of the sediments. Accordingly, for a given sediment with a specific texture, the maximum angle of the depositional slope cannot be higher than its angle of repose (Nemec, 1990). In contrast, shelf-type deltas develop along a depositional profile having an angle less than 5 degrees. (b) Recurrence and magnitude of the fault activity play a major role in the evolution of fault-controlled systems since the creation of accommodation as well as the balance between depth ratio and sediment supply have an impact on the depth ratio. (c) High versus low depth-ratio defines if the hanging wall deposits

are likely attached or not to their footwall counterpart. In case of an extremely low depth-ratio as interpreted for the studied sections, the systems are characterised by a bypass zone along the fault scarp with sediments accumulated to form an unsteady base-of-scarp deposit. (iv) Finally, the accommodation versus sediment supply controls the achievement of conditions such that an unsteady-state system may evolve into steady state and vice versa through time.

As reported by Bell, Duclaux, Nixon, Gawthorpe, and McNeill (2018) for the Corinth Rift, amagmatic rifts not affected by pre-existing low-angle structures like the Crati and Messina rifts accommodate strain along high-angle faults (dipping >30 degrees). Only a progressive accumulation of sediments as base-of-scarp deposits could set the equilibrium conditions (e.g. required angle of the depositional slope and high depth-ratio) to promote sediment accumulation in a steady state. Equilibrium conditions are controlled by the activity of the margin faults and their balance against sediment supply. In the study areas, several works (e.g. Colella, 1988b; Ghisetti, 1992; Roda-Boluda & Whittaker, 2017; Spina et al., 2011) document that faults have been active during deposition supporting that they have been crucial into the development of the unsteady base-of-scarp deposits and their evolution towards a steady state and vice versa. Unfortunately, there are no data to constrain possible palaeodepth estimations for the lower portion of the Civita section. However, ecological information referred to the bioclasic fraction (i.e. coral fragments) recognised in the Croce Valanidi and San Teodoro sections suggest that the lower portion of the Vinco Calcarenites Fm accumulated in a bathyal condition with the step fault scarp working as bypass area.

For an unsteady base-of-scarp system to reach a steady state (Figure 14), sedimentation at the apex has to aggrade up or above the base level and the depositional slope to decrease to a critical angle (Nemec, 1990). Depending upon the rates of fault slip and sediment supply, the unsteady systems can evolve through time into two possible scenarios. (a) At a relatively low fault-slip rate or high-sediment supply, the base-of-scarp deposit may exhaust the tectonically created accommodation and evolve into steady-state Gilbert-type or shoal-water delta (Figure 14), thus moving towards the base of the BGS triangle (Figure 2) while passing through transitional unsteady states. (b) At a relatively high fault-slip rate or low sediment supply, the base-of-scarp deposit will be subject to protracted subaqueous aggradation and progradation remaining in an unsteady -state.

7 | CONCLUSIONS

Base-of-scarp deposits represent unsteady-state systems showing primary inclined bedding and aggradational to progradational geometries along active fault scarps. Base-of-scarp deposits form entirely subaqueously without a direct depositional connection with their subaerial or shallower counterpart located on the footwall. The non-depositional sector separating the source area from the base-of-scarp deposits represents a sediment bypass zone. The bedding geometry and spatial grain-size trend of base-of-scarp systems (B) differ markedly from those of the fault-controlled common Gilbert-type (G) and shoal-water (S) deltas. Main characteristic aspects consist of (a) progressive upwards decrease in strata dip, (b) low depth-ratio, (c) immature texture of the basal deposits evolving upward into slightly more mature and organized beds, (d) a fining-upward general trend and (e) dynamic evolution from unsteady- to steady-state systems and vice versa.

On this basis, base-of-scarp systems can be distinguished from possible erosional relics of Gilbert-type or shoal-type deltas in the stratigraphic record. As a rule, the base-of-scarp systems can reach a steady state of development by evolving into a Gilbert-type (G) or shoal-water (S) delta once the sediment supply eventually outpaces accommodation. Accordingly, sediment accumulation and related change into the depositional slope angle guide the system towards a new depositional style without any major change in the basin physiography.

ACKNOWLEDGEMENTS

This research is part of the 'Fault-Controlled Deposits - Phase I' Joint Industry Project sponsored by AkerBP, DNO, Neptune Energy and Spirit Energy, which support the CSI (Clastic Sedimentology Investigation) research group. We thank W. Nemec for reading through an earlier version of this manuscript. The authors acknowledge the Associate Editor, Craig Magee, and Reviewers, Tim Cullen and Mark Ireland for their constructive and detailed reviews which greatly improved the manuscript.

CONFLICT OF INTEREST

The authors have no conflict of interest to declare.

DATA AVAILABILITY STATEMENT

The data that support the findings of this study are available from the corresponding author upon request.

ORCID

Domenico Chiarella https://orcid.org/0000-0003-2482-0081

REFERENCES

Abeyta, A., & Paola, C. (2015). Transport dynamics of mass failures along weakly cohesive clinoform foresets. *Sedimentology*, *62*, 303–313.

Barrett, B.,Collier, R. E. L. L., Hodgson, D. M., Gawthorpe, R. L., Dorrell, R. M., & Cullen, T. M. (2019). Quantifying faulting and base level controls on syn-rift sedimentation using stratigraphic

architectures of coeval fan deltas: Constraining Early-Middle Pleistocene baselevel amplitude change in Lake Corinth. *Basin Research*, *31*, 1040–1065.

Barrier, P. (1986). Evolution paleogeographic du detroit de Messine au Pliocene et au Pleistocene. *Giornale Di Geologia*, *48*, 7–24.

Barrier, P., Di Geronimo, L., & Lanzafame, G. (1986). I rapporti tra tettonica e sedimentazaione nell'evoluzione recente dell'Aspromonte Occidentale. *Rivista Italiana Paleontologia E Sedimentologia*, *91*, 537–556.

Bell, R. E., Duclaux, G., Nixon, C. W., Gawthorpe, R. L., & McNeill, L. C. (2018). High-angle, not low-angle, normal faults dominate early rift extension in the Corinth Rift, central Greece. *Geology*, *46*, 115–118. https://doi.org/10.1130/G39560.1

Blikra, L. H., & Nemec, W. (1998). Postglacial colluvium in western Norway: Depositional processes, facies and paaeoclimatic record. *Sedimentology*, *45*, 909–959.

Catalano, R., Monaco, C., & Tansi, C. (1993). Pleistocene strike-slip tectonics in the Lucanian Apennine (Southern Italy). *Tectonics*, *12*, 56–65.

Catalano, S., De Guidi, G., Monaco, C., Tortorici, G., & Tortorici, L. (2008). Active faulting and seismicity along the Siculo-Calabrian Rift Zone (Southern Italy). *Tectonophysics*, *453*, 177–192.

Chiarabba, C., Agostinetti, N. P., & Bianchi, I. (2016). Lithospheric fault and kinematic decoupling of the Apennines system across the Pollino range. *Geophysical Research Letters*, *43*, 3201–3207.

Chiarella, D. (2016). Angular and tangential toeset geometry in tidal cross strata: an additional feature of current-modulated deposits. In B. Tessier, & J.-Y. Reynaud (Eds.), *Contributions to modern and ancient tidal sedimentology: Proceedings of the tidalites 2012 conference* (pp. 185–195). Hoboken, NJ: IAS Special Publication. https://doi.org/10.1002/9781119218395.ch10

Chiarella, D., & Longhitano, S. G. (2012). Distinguishing depositional environments in shallow-water mixed, bio-siliciclastic deposits on the basis of the degree of heterolithic segregation (Gelasian, southern Italy). *Journal of Sedimentary Research*, *82*, 969–990. https://doi.org/10.2110/jsr.2012.78

Chiarella, D., Longhitano, S., Sabato, L., & Tropeano, M. (2012). Sedimentology and hydrodynamics of mixed (siliciclastic-bioclastic) shallow-marine deposits of Acerenza (Pliocene, Southern Apennines, Italy). *Italian Journal of Geosciences*, *131*, 136–151.

Chiarella, D., Longhitano, S. G., & Tropeano, M. (2017). Types of mixing and heterogeneities in mixed siliciclastic-carbonate sediments. *Marine and Petroleum Geology*, *88*, 617–627.

Chiarella, D., Longhitano, S. G., & Tropeano, M. (2019). Different stacking patterns along an active fold-and-thrust belt—Acerenza Bay, Southern Apennines (Italy). *Geology*, *47*, 139–142. https://doi.org/10.1130/G45628.1

Colella, A. (1988a). Fault-controlled marine Gilbert-type fan deltas. *Geology*, *16*, 1031–1034. https://doi.org/10.1130/0091-7613(1988)016<1031:FCMGTF>2.3.CO;2

Colella, A. (1988b). Pliocene-Holocene fan deltas and braid deltas in the Crati basin: A consequence of varying tectonic conditions. In W. Nemec, & R. J. Steel (Eds.), *Fan deltas: sedimentology and tectonic settings* (pp. 50–74). LondonBlackie and Son Ltd.

Cullen, T. M., Collier, R. E. L. L., Gawthorpe, R. L., Hodgson, D. M., & Barrett, B. J. (in press). Axial and transverse deep-water sediment supply to syn-rift fault terraces: Insights from the West Xylokastro Fault Block, Gulf of Corinth, Greece. *Basin Research*. https://doi.org/10.1111/bre.12416

Dorsey, R. J., Umhoefer, P. J., & Renne, P. R. 1995. Rapid subsidence and stacked Gilbert-type fan deltas, Pliocene Loreto basin, Baja California Sur, Mexico. *Seidmentary Geology*, *98*, 181–204.

Ethridge, F., & Wescott, W. (1984). Tectonic setting, recognition and hydrocarbon reservoir potential of fan-delta deposits. In E. H. Koster, & R. J. Steel (Eds.), *Sedimentology of gravels and conglomerates*, (Vol. *10*, pp. 217–235). Calgary, Canada: CSPG Special Publications.

Ferranti, L., Santoro, E., Mazzella, M. E., Monaco, C., & Morelli, D. (2009). Active transpression in the northern Calabria Apennines, southern Italy. *Tectonophysics*, *476*, 226–251.

Filice, F., & Seeber, L. (2019). The culmination of an oblique time-transgressive arc continent collision: The Pollino Massif between Calabria and the Southern Apennines, Italy. *Tectonics*, *38*, 3261–3280. https://doi.org/10.1029/2017TC004932

Garcia-Garcia, F., Fernandez, J., Viseras, C., & Soria, J. M. (2006). Architecture and sedimentary facies evolution in a delta stack controlled by fault growth (Betic Cordillera, southern Spain, late Tortonian). *Sedimentary Geology*, *185*, 79–92. https://doi.org/10.1016/j.sedgeo.2005.10.010

Ghisetti, F. (1979). Evoluzione neotettonica dei principali sistemi di faglie della Calabria centrale. *Bollettino Della Società Geologica Italiana*, *98*, 387–430.

Ghisetti, F. (1984). Recent deformations and the seimogenic source in the Messina Strait (Southern Italy). *Tectonophysics*, *109*, 191–208.

Ghisetti, F. (1992). Fault parameters in the Messina Strait (southern Italy) and relations with the seismogenic source. *Tectonophysics*, *210*, 117–133. https://doi.org/10.1016/0040-1951(92)90131-O

Ghisetti, F., & Vezzani, L. (1982). Strutture tensionali e compressive indotti da meccanismi profondi lungo la linea del Pollino (Appennino meridionale). *Bollettino Della Società Geologica Italiana*, *101*, 385–440.

Gobo, K., Ghinassi, M., & Nemec, W. (2015). Gilbert-type deltas recording short-term base-level changes: Delta-brink morphodynamics and related foreset facies. *Sedimentology*, *62*, 1923–1949. https://doi.org/10.1111/sed.12212

Hardy, S., Dart, C. J., & Waltham, D. (1994). Computer modelling of the influence of tectonics on sequence architecture of coarse-grained fan deltas. *Marine and Petroleum Geology*, *11*, 561–574. https://doi.org/10.1016/0264-8172(94)90068-X

Henstra, G. S., Grundvåg, S. A., Johannessen, E. P., Kristensen, T. B., Midtkandal, I., Nystuen, J. P., … Windelstad, J. (2016). Depositional processes and stratigraphic architecture within a coarse-grained rift-margin turbidite system: The Wollaston Forland Group, east Greenland. *Marine and Petroleum Geology*, *76*, 187–209. https://doi.org/10.1016/j.marpetgeo.2016.05.018

Jia, Y., Lin, C., Eriksson, K. A., Niu, C., Li, H., & Zhang, P. (2019). Fault control on depositional systems and sequence stratigraphic architecture in a multiphase, rifted, lacustrine basin: A case study from the paleogene of the central Bohai Bay Basin, Northeast China. *Marine and Petroleum Geology*, *101*, 459–475. https://doi.org/10.1016/j.marpetgeo.2018.12.019

Jopling, A. V. (1965). Hydraulic factors controlling the shape of the laminae in laboratory deltas. *Journal of Sedimentary Petrography*, *35*, 777–791.

Lai, S. Y. J., Hsiao, Y.-T., & Wu, F.-C. (2017). Asymmetric effects of subaerial and subaqueous basement slopes on self-similar morphology of prograding deltas. *Journal of Geophysical Research: Earth Surface*, *122*, 2506–2526. https://doi.org/10.1002/2017JF004244

Leeder, M. R., & Gawthorpe, R. L. (1987) Sedimentary models for extensional tilt-block/half-graben basins. In M. P. Coward, J. F. Dewey, & P. L. Hancock (Eds.), Continental extensional tectonics. *Geological Society, London, Special Publications*, *28*, 139–152.

Lewis, M. M., Jackson, C.-A.-L., Gawthorpe, R. L., & Whipp, P. S. (2015). Early synrift reservoir development on the flanks of extensional forced folds: A seismic-scale outcrop analog from the Hadahid fault system, Suez Rift, Egypt. *AAPG Bulletin*, *99*, 985–1012. https://doi.org/10.1306/120111414036

Longhitano, S. G. (2008). Sedimentary facies and sequence stratigraphy of coarse-grained Gilbert-type deltas within the Pliocene thrust-top Potenza Basin (Southern Apennines, Italy). *Sedimentary Geology*, *210*, 87–110. https://doi.org/10.1016/j.sedgeo.2008.07.004

Longhitano, S. G. (2018). Between Scylla and Charybdis: The sedimentary dynamics of the ancient, Early Pleistocene Messina Strait (central Mediterranean) based on its modern analogue. *Earth-Science Reviews*, *179*, 248–286.

Longhitano, S. G., Chiarella, D., Di Stefano, A., Messina, C., Sabato, L., & Tropeano, M. (2012). Tidal signatures in Neogene to Quaternary mixed deposits of southern Italy straits and bays. *Sedimentary Geology*, *279*, 74–96. https://doi.org/10.1016/j.sedgeo.2011.04.019

Longhitano, S. G., Chiarella, D., & Muto, F. (2014). Three-dimensional to two-dimensional cross-strata transition in the lower Pleistocene Catanzaro tidal strait transgressive succession (southern Italy). *Sedimentology*, *61*, 2136–2171. https://doi.org/10.1111/sed.12138

Longhitano, S. G., Sabato, L., Tropeano, M., Murru, M., & Carannante, G. (2015). Outcrop reservoir analogous and porosity changes in continental deposits from an extensional basin: The case study of the upper Oligocene Sardinia Graben System, Italy. *Marine and Petroleum Geology*, *67*, 439–459. https://doi.org/10.1016/j.marpetgeo.2015.05.022

Massari, F. (1996). Upper-flow-regime stratification types on steep-face, coarse-grained, Gilbert-type progradational wedges (Pleistocene, southern Italy). *Journal of Sedimentary Research*, *66*, 364–375. https://doi.org/10.1306/D426834C-2B26-11D7-8648000102C1865D

Massari, F., & Chiocci, F. L. (2006). Biocalcarenite and mixed cool-water prograding bodies of the Mediterranean Pliocene and Pleistocene: architecture, depositional setting and forcing factors. *Geological Society, London, Special Publications*, *255*(1), 95–120. https://doi.org/10.1144/GSL.SP.2006.255.01.08

Massari, F., & Colella, A. (1988). Evolution and types of fan-delta systems in some major tectonic settings. In W. Nemec, & R. J. Steel (Eds.), *Fan Deltas: Sedimentology and Tectonic Settings* (pp. 103–122). LondonBlackie and Son Ltd.

Miall, A. D. (1976). Facies model 4, deltas. *Geoscience Canada*, *3*, 215–227.

Monaco, C., & Tansi, C. (1992). Strutture transpressive lungo la zona trascorrente sinistra nel versante orientale del Pollino (Appennino calabro-lucano) (Transpressional structures along the left-lateral strike-slip zone on the eastern slope of Mt. Pollino (Calabrian-Lucanian Apennine)). *Bollettino Della Societ a Geologica Italiana*, *111*, 291–301.

Monaco, C., & Tortorici, L. (2000). Active faulting in the Calabrian arc and eastern Sicily. *Journal of Geodynamics*, *29*, 407–424. https://doi.org/10.1016/S0264-3707(99)00052-6

Monaco, C., Tortorici, L., Nicolich, R., Cernobori, L., & Costa, M. (1996). From collisional to rifted basins: An example from the southern Calabrian arc (Italy). *Tectonophysics*, *266*, 233–249. https://doi.org/10.1016/S0040-1951(96)00192-8

Nalin, R., Ghinassi, M., Foresi, L. M., & Dallanave, E. (2016). Carbonate Deposition in restrcited basins: A Pliocene case study from central Mediterranena (Northwestern Apennines). *Journal of Sedimentary Research*, *86*, 1–32.

Nemec, W. (1990) Aspects of sediment movement on steep delta slopes, In A. Colella, & D. B. Prior (Eds.), Coarse-Grained Deltas. *IAS Special Publication*, *10*, 29–73.

Ono, K., & Plink-Björklund, P. (2018). Froude supercritical flow bedforms in deepwater slope channels? Field Examples in Conglomerates, Sandstones and fine-grained Deposits. *Sedimentology*, *65*, 639–669. https://doi.org/10.1111/sed.12396

Pepe, M., & Gallicchio, S. (2013). Shallow-marine systems in a wedge-top basin setting: An example from the middle-upper Pliocene deposits of the Southern Apennines mountain front (Basilicata region, South Italy). *Italian Journal of Geosciences*, *132*, 304–320. https://doi.org/10.3301/IJG.2012.32

Postma, G., Lang, J., Hoyal, D. C., Fedele, J. J., Demko, T., Abreu, V., & Pederson, K. H. (in press) Reconstruction of bedform dynamics controlled by supercritical flow in the channel–lobe transition zone of a deep-water delta (Sant Llorencß del Munt, northeast Spain, Eocene). *Sedimentology*. https://doi.org/10.1111/sed.12735

Postma, G., Nemec, W., & Kleinspehn, K. L. (1988). Large floating clasts in turbidites: A mechanism for their emplacement. *Sedimentary Geology*, *58*, 47–61. https://doi.org/10.1016/0037-0738(88)90005-X

Prior, D. B., & Bornhold, B. D. (1988). Submarine morphology and processes of fjord fan deltas and related high-gradient systems: Modern examples from British Columbia. In W. Nemec, & R. J. Steel (Eds.), *Fan deltas: sedimentology and tectonic settings* (pp. 103–122). LondonBlackie and Son Ltd.

Roda-Boluda, D. C., & Whittaker, A. C. (2017). Structural and geomorphological constraints on active normal faulting and landscape evolution in Calabria, Italy. *Journal of the Geological Society*, *174*, 701–720.

Rossi, V. M., Longhitano, S. G., Mellere, D., Dalrymple, R. W., Steel, R. J., Chiarella, D., & Olariu, C. (2017). Interplay of tidal and fluvial processes in an early Pleistocene, delta-fed strait margin (Calabria, Southern Italy). *Marine and Petroleum Geology*, *87*, 14–30. https://doi.org/10.1016/j.marpetgeo.2017.02.021

Sorriso-Valvo, M., & Terranova, O. (2006). The Calabrian fiumara streams, Zeitschrift für Geomorphologie. *Supplementband*, *143*, 109–125.

Spina, V., Tondi, E., & Mazzoli, S. (2011). Complex basin development in a wrench-dominated back-arc area: Tectonic evolution of the Crati Basin, Calabria, Italy. *Journal of Geodynamics*, *51*, 90–109. https://doi.org/10.1016/j.jog.2010.05.003

Steel, R. J., Moehle, S., Nilson, H., Roe, S. L., & Spinnangre, A. (1977). Coarsening upwards cycles in the alluvium of Homelen Basin (Devonian), Norway: Sedimentary response to tectonic events. *Bulletin of the Geological Society of America*, *88*, 1124–1134.

Stevenson, C. J., Jackson, C. A. L., Hodgson, D. M., Hubbard, S. M., & Eggenhuisen, J. T. (2016). Deep water sediment bypass. *Journal of Sedimentary Research*, *85*, 1058–1081. https://doi.org/10.2110/jsr.2015.63

Surlyk, F. (1984). Fan-delta to submarine fan conglomerates of the Volgian-Valanginian Wollaston Forland group, east Greenland. In E. H. Koster, R. J. Steel (Eds.), Sedimentology of Gravels and

Conglomerates. *Canadian Society of Petroleum Geologists Memoir*. *10*, 359e382.

Tansi, C., Folino, G. M., Muto, F., Perrotta, P., Russo, L., & Critelli, S. (2016). Seismotectonics and landslides of the Crati Graben (Calabrian Arc, Southern Italy) 2016. *Journal of Maps*, *12*, 363–372.

Tansi, C., Muto, F., Critelli, S., & Iovine, G. (2007). Neogene-Quaternary strike-slip tectonics in the central Calabrian Arc (southern Italy). *Journal of Geodynamics*, *43*, 393–414. https://doi.org/10.1016/j.jog.2006.10.006

Tripodi, V., Muto, F., Brutto, F., Perri, F., & Critelli, S. (2018). Neogene-Quaternary evolution of the forearc and backarc regions between the Serre and Aspromonte Massifs, Calabria (southern Italy). *Marine and Petroleum Geology*, *95*, 328–343. https://doi.org/10.1016/j.marpetgeo.2018.03.028.

Turco, E., Maresca, R., & Cappadona, P. (1990). La tettonica plio-pleistocenica del confine calabro-lucano: Modello cinematico (Plio-Pleistocene tectonics at the Calabrian-Lucanian boundary: A kinematic model). *Memorie Della Societ a Geologica Italiana*, *45*, 519–529.

Turner, C. C., & Connell, E. R. (2018). Mid to Late Jurassic Graben margin development and evolution of shallow marine to submarinefan systems in the Brae area south of south Viking Graben, UK North Sea. *AAPG Memoir*, *115*, 163–211.

Van Dijk, J. P., Bello, M., Brancaleoni, G. P., Cantarella, G., Costa, V., Frixa, A., … Zerilli, A. (2000). A regional structural model for the northern sector of the Calabrian Arc (southern Italy). *Tectonophysics*, *324*, 267–320. https://doi.org/10.1016/S0040-1951(00)00139-6

Yesares-García, J., & Aguirre, J. (2004). Quantitative taphonomic analysis and taphofacies in lower Pliocene temperate carbonate-siliciclastic mixed platform deposits (Almeria-Nijar Basin, SE Spain). *Palaeogeography, Palaeoclimatology, Palaeoecology*, *207*, 83–103.

How to cite this article: Chiarella D, Capella W, Longhitano SG, Muto F. Fault-controlled base-of-scarp deposits. *Basin Res*. 2021;33:1056–1075. https://doi.org/10.1111/bre.12505